AIAA-2001-0757
Cryogenic Model Materials (Invited)

W. M. Kimmel, N. S. Kuhn and R. F. Berry
NASA Langley Research Center, Hampton, Virginia

J. A. Newman
U.S. Army Research Laboratory
Vehicle Technology Directorate
Langley Research Center, Hampton, Virginia

39th AIAA Aerospace Sciences Meeting & Exhibit
8-11 January 2001
Reno, Nevada

Cryogenic Model Materials

W. M. Kimmel*, J. A. Newman**, N. S. Kuhn†, and R. F. Berry‡
NASA Langley Research Center
Hampton, Virginia

ABSTRACT

An overview and status of current activities seeking alternatives to 200 grade 18Ni Steel CVM alloy for cryogenic wind tunnel models is presented. Specific improvements in material selection have been researched including availability, strength, fracture toughness and potential for use in transonic wind tunnel testing. Potential benefits from utilizing damage tolerant life-prediction methods, recently developed fatigue crack growth codes and upgraded NDE methods are also investigated. Two candidate alloys are identified and accepted for cryogenic/transonic wind tunnel models and hardware.

INTRODUCTION

Early in the development of the National Transonic Facility (NTF) at Langley Research Center (LaRC), much research was performed to identify and characterize materials suitable for building wind tunnel models and support hardware. These activities have not continued or pursued since the early 1980's. A motivation for these activities has resurfaced in recent years due to the increasing difficulty in procuring 200 grade maraging steel. Due to current trends in the industry, no depots or other vendors maintain stock of this material. This has impacted the costs and development cycle times for almost all NTF research hardware projects and forced a mass buy strategy that is limiting research opportunities.

Additionally, NTF models need to simulate aircraft performance under more severe aerodynamic conditions than in previous decades. Increases in dynamic pressure (Q) and unsteady loading require new materials and techniques to provide increased model performance while eliminating structural failure at the higher static and dynamic loads. Furthermore, models are tested at cryogenic (-275^{o}F) temperature provide high Reynolds number flows. Therefore, model alloys must have desirable a number of other desirable characteristics at cryogenic conditions.

Under high static loads two failure modes exist; yielding and fracture. Model alloys need high tensile strength and fracture toughness to prevent yielding and fracture failures, respectively. Prevention of structural failure under cyclic or fatigue loading is more difficult. Initially, a structure may be known to contain no cracks large enough for failure to occur under anticipated loads. However, under fatigue loading small cracks may grow to a critical size where fracture occurs. To prevent fatigue crack failures a damage tolerant life-prediction method has been developed. Here, fatigue life is assumed equivalent to fatigue crack growth (FCG) from an initial defect to a critical crack size. Life prediction is a function of final and initial crack sizes, anticipated loads, and FCG behavior. Damage tolerance is superior to existing fatigue prevention schemes, in terms of safety and cost of replacement parts, and will be evaluated to ensure safe operation of NTF models. Because reliable detection of small cracks is important, non-destructive evaluation (NDE) techniques will also be studied.

NOMENCLATURE

a,c	crack depth. length
AOA	Angle of attack
C_{VN}	Charpy impact energy
K_{Ic}	plane-strain fracture toughness
N	load cycle count
Q	dynamic pressure
R_e	Reynolds number
R	stress ratio, $\sigma_{max}/\sigma_{min}$
σ_u	ultimate strength
σ_y	yield stress

* Senior Mechanical Engineer, Model Systems Branch, NASA-Langley Research Center, Hampton, VA 23681
** Aerospace Engineer, U.S. Army Research Laboratory, Vehicle Technology Directorate, Hampton, VA 23681
† Aerospace Engineering Co-op Student, NASA-Langley Research Center, University of Wisconsin, Madison
‡ Senior Inspector, Quality Applications Technology Branch, NASA-Langley Research Center, Hampton, VA 23681

OBJECTIVES

The activities presented in this paper seek to achieve the following objectives:

- Solve NTF material supply issues by finding a suitable alternate alloy.
- Find model alloys with higher fracture toughness, ultimate strength and FCG characteristics to safely permit testing at higher static and dynamic loads.
- Predict and manage fatigue lives of models using damage tolerance methods under anticipated wind tunnel loading.
- Revise LaRC wind tunnel model design criteria, LAPG1710.15[1], to implement damage tolerance methods and reduce model development cycle times.
- Evaluate NDE techniques for detection or monitoring small fatigue cracks in potential model alloys.

PROJECT APPROACH

This project was divided into two phases. Phase I sought potential alternatives to grade 200 maraging steel from a list of commercially available alloys. A few alloys were selected based on availability, ease of machining, and material behavior (*i.e*. tensile strength, stiffness, and fracture toughness) at cryogenic and room temperatures. The list of candidate alloys was further narrowed to seven based on available funds (*i.e*. cost). Finally, the list of candidate alloys was reduced to two (Vascomax C250 and Aermet 100) based on results of further mechanical testing.

The objectives of the second phase was to select one of the two candidate alloys based on fatigue crack growth (FCG) and fracture characteristics. FCG and fracture behavior are important because fatigue life predictions are to be made based on damage tolerance methods. Phase II consisted of the following activities:

1. Determine FCG and fracture behavior of Vascomax C250 and Aermet100 at both cryogenic (-275^{o}F) and room temperature (75^{o}F).
2. Use damage tolerance life prediction methods for maraging steel models.
3. Revise LaRC guidance documentation LAPG1710.15 to qualify new alloys and life prediction methods.[1]
4. Evaluate the role of NDE in damage tolerance life management.

NTF materials search (Phase I)

The materials search began with an extensive literature review and discussions with material manufacturers. A comprehensive search for alternate cryogenic model alloys was done by Tobler in 1980.[2] The primary criteria acceptable alternative alloys must satisfy are listed as follows.

1. **Material properties** – possess high fracture toughness and ultimate tensile strength at low (-275°F) temperature.
2. **Metallurgical stability** – permit a stable heat treatment for cryogenic-to-room-temperature thermal cycling.
3. **Availability** – commercially available in stock shapes with short delivery time in bars up to 18” diameter and plates up to 6” x 36” x 72”.
4. **NDE** – can be evaluated by metallurgical and ultrasonic inspection to satisfy LaRC guidance documents.
5. **Machinability** – desirable machining, handling and fabricating characteristics.

Results of Tobler[2], Wigely[3] and Rush[4] indicate nickel maraging steels are best suited to meet the high K_{Ic} and high σ_y requirements of NTF model alloys. Figure 1 is a plot of K_{Ic} versus σ_y for several materials. Most materials shown have properties within the shaded region. The most desirable properties (high K_{Ic} and high σ_y) lie along the upper bound of this shaded region. (As seen in the lower right corner of the figure, Vascomax C250 and Aermet 100 are slightly above the shaded region.) However, maraging steels are primarily used for aerospace and nuclear applications and are somewhat difficult to obtain due to limited demand. The phase I study narrowed the list of candidate alloys to the following seven:

1. G90c© – (British Steel)
2. 13-8 Supertough© – (Allvac)
3. C250 Maraging – (Allvac, Carpenter)
4. T200© – (Allvac)
5. Custom465© – (Carpenter)
6. Aermet100© – (Carpenter)
7. PH13-8Mo – (various manufacturers)

Each of the seven alloys were ordered and delivered in an acceptable time. Specimens were machined and sent to a certified lab for Charpy impact tests (ASTM E-96), tensile tests (ASTM E-23) and thermal expansion tests (ASTM E-370). Charpy impact energy and ultimate tensile

strength for each material are listed in Table 1. The results of this phase I study were presented at an NTF workshop in the fall of 1999. As indicated by highlighted portions of Table 1, Aermet100© and C250 were chosen for additional study in Phase II. This decision was based on ultimate tensile stress, availability, and fracture toughness.

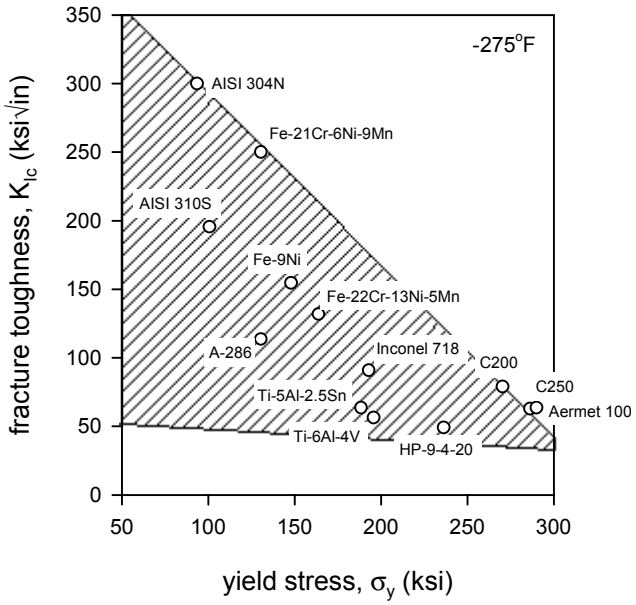

Figure 1 – Plot of K_{Ic} versus σ_y for several alloys.

In previous literature, C250 and AF1410 were identified as potential alloys that would be usable for cryogenic models. Microstructural stability tests were favorable and included in the findings of Tobler[2] and Wigely[3]. However, these two alloys were not initially accepted for NTF models. Instead, Grade 200 maraging steel was selected because of higher plane-strain fracture toughness (K_{Ic}) at cryogenic temperature. Subsequent to phase I, it was discovered that Aermet100© is essentially a reformulation of the AF1410 alloy produced by Carpenter Steel corporation.

Table 1 – Material properties of Phase I alloys.

Material	C_{vn} (ft-lb)	σ_u (ksi)
13-8	27.8	203.2
Aermet 100	16.9	300.3
Custom 465	5.2	268.1
T200	24.3	276.6
C250	14.1	305.3
13-8 Supertough	117.0	215.0
G90c	21.1	279.7

The extraordinarily high Charpy impact energy of 13-8 Supertough© initially made it an attractive candidate. This alloy is similar to Ph13-8Mo, which was previously found to be acceptable for cryogenic testing although care must be taken to overcome cryogenic instability related to formation of unstable austenite during heat treatment[5]. This material is available in limited production sizes and has a modest ultimate strength. Thus, 13-8 Supertough© was not selected for further consideration.

NTF materials study (Phase II)

Phase II began in spring 2000 and is scheduled to be complete by February 2001. In this phase, FCG and fracture behavior of both alloys (Vascomax C250 and Aermet100©) will be determined to enable fatigue-life prediction and management by damage tolerance techniques. Currently, most of phase II is completed. Finally, non-destructive evaluation (NDE) techniques will be tested on specimens to determine the smallest detectable crack size. The ability to detect or monitor propagating fatigue cracks is an important step towards applying damage tolerance methods.

Experimental testing and results

Existing cracks are known to grow under cyclic, or fatigue loading. In fact, a significant portion of the fatigue lives of most engineering structures is spent propagating small cracks to failure.[6] Damage tolerance life prediction methods are based on FCG behavior and are superior to older "safe-life" life prediction methods, in terms of safety and part replacement costs.[7] Using damage tolerance to prevent fatigue failure requires (1) knowledge of how fatigue cracks propagate to failure and (2) the ability to monitor propagating fatigue cracks. FCG behavior of Vascomax C250 and Aermet 100© will be discussed in this section. NDE tests to detect and monitor fatigue cracks are discussed later.

FCG data obtained from laboratory specimens is related to crack behavior in other components using the cyclic range of stress intensity factor, ΔK, as a crack-tip driving force. Although ΔK is a function of cyclic stress and crack length, cracks subjected to the same ΔK have nearly identical fatigue crack growth rates (average increment of crack growth per cycle). FCG tests were performed on both candidate alloys following ASTM standards (E647). A computer-controlled system[8] was used to continuously monitor crack length throughout testing using compliance data from a clip gage.[9] This system automatically

adjusts loads as the crack grows to ensure that programmed stress intensity factors are applied throughout the tests. This allows FCG tests to be performed with controlled ΔK. As outlined in ASTM E647, FCG tests were performed where ΔK was gradually changed as the crack propagated. In this way, the relationship between fatigue crack growth rate and ΔK can be determined more efficiently. Two types of FCG tests were performed in this study. Traditionally, FCG tests are performed where the load ratio (ratio of minimum to maximum load, R) remains constant as ΔK is changed. Constant K_{max} tests were also used for decreasing ΔK tests. For these tests, ΔK is reduced by increasing the minimum value of stress intensity. Constant K_{max} tests are desirable because FCG threshold (that is, values of ΔK where fatigue crack growth rates approach zero) achieved during constant-R, reducing ΔK tests are associated with artificially high crack closure levels.[10-11] Constant K_{max} test data at low ΔK is free of closure, and is used to characterize the growth of small cracks in model alloys at low ΔK.[12]

Both materials were obtained in forged round bars of approximately 6" diameter. Each material was commercially available in this shape and delivered within 2 weeks of order. Disk-shaped compact tension specimens were made from 1" thick slices of the round bars (see ASTM standard E399).

FCG data is presented in Figure 2 for Vascomax C250 and Aermet 100 as FCG rate versus ΔK. (Note that log-log axes are used, which is typical of FCG data.) Curves are fit through the data for each material at both cryogenic (-275°F) and room temperature (75°F). Each specimen was precracked at R = 0.1 and ΔK = 15 or 20 ksi√in

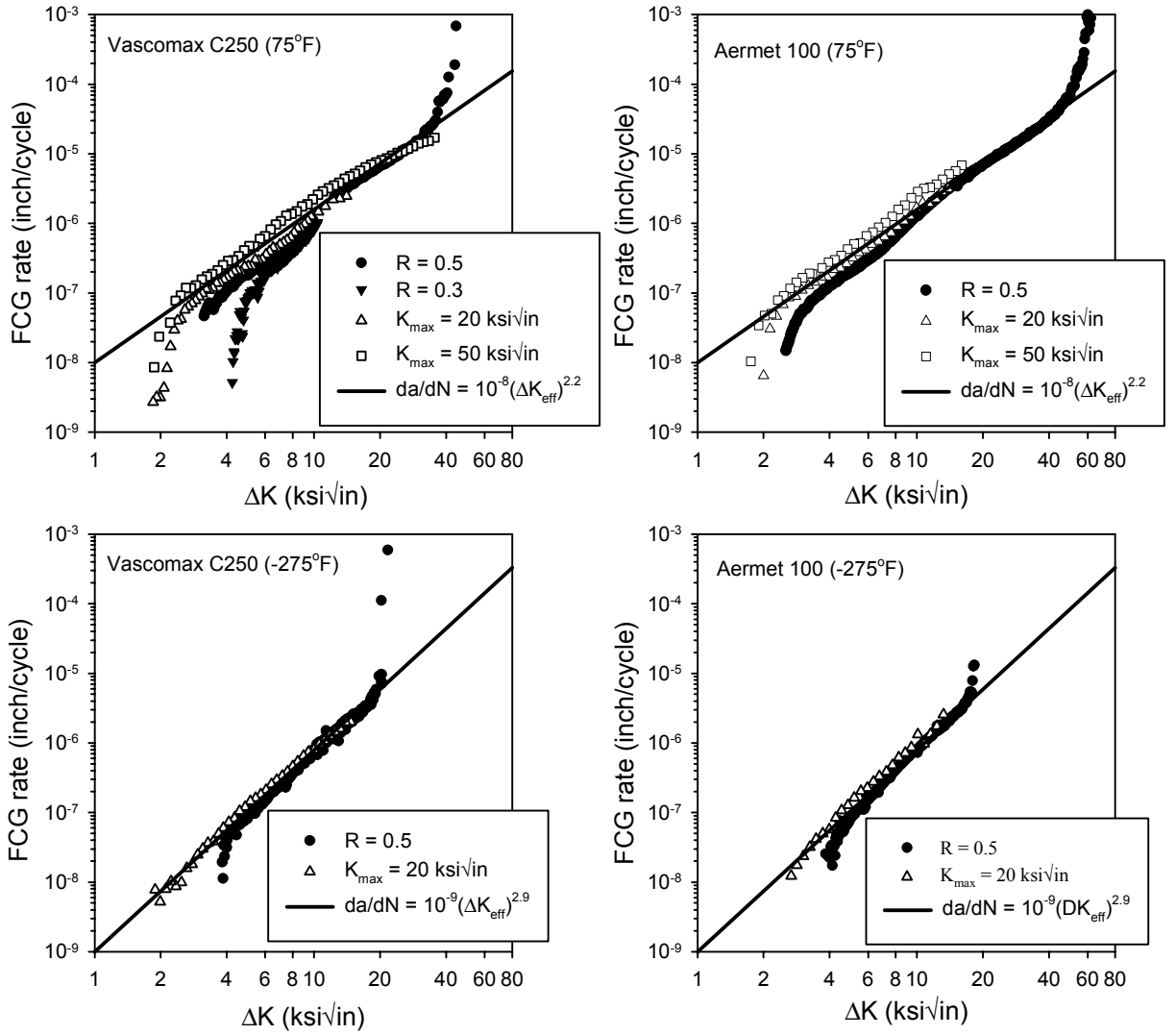

Figure 2 – Fatigue crack growth data for Vascomax C250 and Aermet 100 at 75°F and –275°F.

before FCG testing. Data below and above the precracking loads were achieved by reducing and increasing ΔK during testing, respectively.

FCG data for both Vascomax C250 and Aermet 100 are plotted as FCG rate versus ΔK on the left and right sides of Figure 2, respectively. (Note the use of logarithmic axes.) Data generated at 75°F and –275°F are shown separately. Both constant R and constant K_{max} test data are shown as symbols (refer to legend). An "upper bound" line, shown as a solid line, is fit through the data. This linear relationship (shown in the legends) will later be used for damage tolerance life predictions. The line is a good fit to the data at intermediate values of ΔK (5 ksi$\sqrt{in}$ < ΔK < 20 ksi$\sqrt{in}$). In this range of ΔK, called Paris regime FCG, the relationship between FCG rate and ΔK is nearly linear. At ΔK < 5 ksi$\sqrt{in}$, the FCG rate is much less than an extrapolation of the linear behavior would predict. Here, FCG rates decrease towards an apparent threshold, below which no significant FCG occurs. However, neglecting the fatigue life advantages of FCG threshold will lead to conservative life predictions and greatly simplify life analyses. As ΔK increases, FCG rates increase rapidly as K_{max} approaches the fracture toughness and fracture is immanent. The fracture criterion of damage tolerance analyses will account for this deviation in FCG behavior.

It should be noted that both materials have nearly the same FCG response under similar conditions. That is the linear fit for both materials at 75°F and -275°F are identical. Also these data agree with previous results of C200 steel presented by Wagner[13]. Therefore, no significant difference in FCG performance is expected between these alloys. The only clear difference in these alloys is the cyclic fracture toughness, *i.e.* the ΔK and K_{max} at fracture. Although not a standard fracture toughness test, the data in Figure 2 indicates that Aermet 100 has an edge over C250. Fracture toughness tests are planned for both alloys, but results are not currently available. Existing fracture toughness data for C200 and C250 steels are plotted in Figure 3 as a function of temperature.[14] C200 is tougher at room temperature, but no appreciable advantage is seen at cryogenic temperatures. Based on FCG data in Figure 2, Aermet 100 is expected to outperform both C200 and C250.

Because fracture toughness generally decreases with decreasing temperature, FCG rates at –275°F were expected to be faster than at 75°F. However, the opposite was shown to occur. Comparison of FCG data in Figure 2 indicates that FCG rates were faster at room temperature by approximately a factor of 2. This observation is congruent results on C200 steel by Wagner.[13]

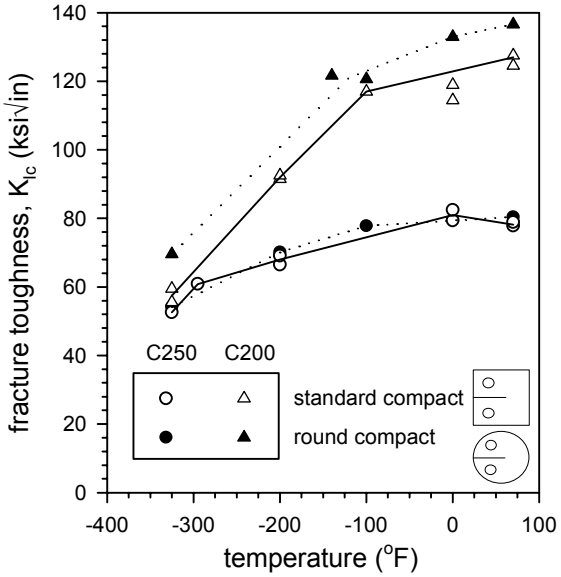

Figure 3 – Fracture toughness vs temperature.

Based on known FCG and fracture data, worst-case FCG conditions occur at 75°F and worst-case fracture performance occurs at –275°F. Fortunately, the current LaRC practice for crack growth life analysis of NTF models uses cryogenic fracture toughness properties and room temperature FCG data, which is conservative. To simplify damage tolerance life prediction and ensure conservative results, life predictions will be made using cryogenic fracture data and room temperature FCG data. Furthermore, the same FCG relation can be used for all model alloys studied here.

This should greatly simplify damage tolerance analyses because only a single FCG relation is needed. Currently, analyses require material specific data normally obtained by a series of expensive and time-consuming tests. Typically, data is not available until late stages of model development, even after the design stage. Although material specific fracture data is still needed, these tests require much less test time than FCG tests. Development and use of a generalized FCG curve should greatly reduce the complexity of performing damage tolerant life analyses on NTF wind tunnel models. It should be reasonable to expect that a fatigue crack-growth

life analysis be performed by the design activity early in the model development process.

DAMAGE TOLERANCE ANALYSES

An increasing number of structures are designed and safely managed using damage tolerance methods. Here, initial defects or cracks are assumed to exist even before fatigue loads are applied. Fatigue life is assumed equivalent to FCG between initial and critical crack sizes, where fracture occurs. Fatigue lives are predicted using FCG and fracture mechanics parameters (such as ΔK and K_{Ic}), which are related to anticipated loads. Fatigue life predictions are made by integrating FCG relations (FCG rate, or da/dN, as a function of ΔK) to estimate the number of cycles until a crack grows to fracture. Several inspection intervals are normally scheduled within the expected fatigue life to ensure an inspection process has multiple chances to detect growing fatigue cracks before failure. Examples of FCG relations are given in Equations 1-3. The linear relation associated with Paris[15] is shown in Equation 1. The Paris relation has the advantage and disadvantages of simplicity. It greatly simplifies fatigue life calculations, but does not consider non-linear effects of FCG threshold or fracture toughness. If the anticipated loads and crack lengths do not produce a ΔK near the FCG threshold, the Paris relation may be adequate. More complicated relationships have been developed by others including Forman[16] (Equation 2) and Newman, as part of a FCG code NASGRO,[17] (Equation 3). The Forman equation accounts for non-linear effects associated with fracture and the NASGRO equation accounts for both threshold and fracture effects.

$$\frac{da}{dN} = C(\Delta K)^m \tag{1}$$

$$\frac{da}{dN} = \frac{A(\Delta K)^n}{(1-R)K_{Ic} - \Delta K} \tag{2}$$

$$\frac{da}{dN} = C\left[\left(\frac{1-f}{1-R}\right)\Delta K\right]^n \frac{\left(1-\frac{\Delta K_{th}}{\Delta K}\right)^p}{\left(1-\frac{K_{max}}{K_c}\right)^q} \tag{3}$$

The NASGROW equation (Equation 3) provides a good approximation of the entire FCG relation from threshold to fracture. As schematically shown in Figure 4, the FCG curve has a sigmoidal shape (S-shaped) and is normally divided into three regions (Stage I –threshold, Stage II – Paris, and Stage III – crack instability). Details of FCG behavior can be found in the literature.[6,16,18,19] Several commercially available FCG software programs have been developed that use FCG relations to make damage tolerance fatigue crack growth predictions.

Fatigue crack growth codes

Five FCG codes were used to analyze two crack problems in NTF hardware under two different load spectra. The FCG codes used included AFGROW 4.0,[20] FASTRAN,[21] Fracture,[22] FractureGraphic 2.1,[23] and NASGRO 3.0.[17] Predictions made by these codes for identical crack configurations and loads are compared.

AFGROW and NASGRO are available to the public and can be obtained over the internet at no cost. FASTRAN (by Jim Newman) and Fracture (by Mike Hudson and Charles Dunton) are codes developed at LaRC. Fracture has previously been used for life predictions of NTF models. FractureGraphic (FG) is a commercially licensed software code. All five codes calculate FCG using a variety of crack configurations, each with a specific stress intensity factor solution (K solution). K solutions define the crack-tip stress intensity factor in terms of crack configuration and loading. It is noteworthy that NASGRO, AFGROW, and FG all share a common material property database, originally compiled for the NASA/FLAGRO computer program in 1986.[24] This database

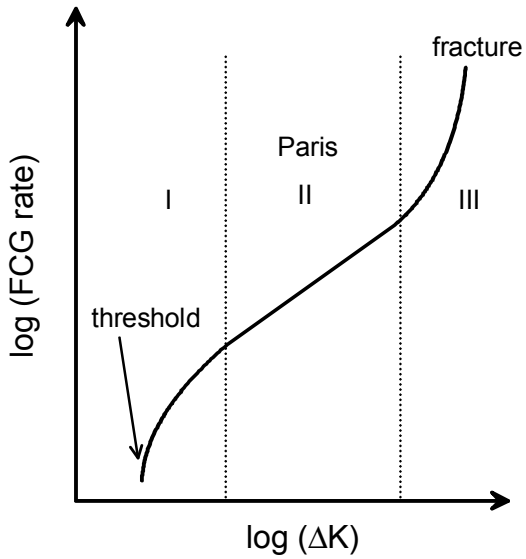

Figure 4 – Typical fatigue crack growth behavior

includes properties for many materials, including maraging steels used for NTF wind tunnel models. FASTRAN incorporates nonlinear or plastic strain material behavior and load interaction effects (acceleration or retardation) using a crack closure concept. These features are unique to FASTRAN and allow more accurate life predictions.

Each of these five FCG codes could be used in the design process of NTF models. However, each code uses different means (*e.g*. different FCG relations and K solutions) to make fatigue life predictions so each code is expected to predict a slightly different result. It is the responsibility of the designer to ensure that the appropriate material relationships are used for a given application. For example, NTF models and hardware are typically subjected to fatigue loads at low ΔK and high K_{max}. Therefore, it is more important to use a FCG relationship with a precise description of threshold than one with a good description of Stage III crack growth.

Load spectra

Traditionally, damage tolerance analyses of NTF models investigated two loading scenarios. The first is a peak load condition that is analogous to the maximum load during an AOA sweep in the wind tunnel at constant dynamic pressure (Q). This AOA sweep is referred to as a "polar." The second loading scenario deals with oscillatory loads (*i.e*. fatigue loading) during testing. FCG data at load ratios of 0 and 0.6 (25% above and below the mean stress) are used to model the effects of peak and oscillatory loading, respectively. In this way, effects of an entire load spectrum is predicted using two constant amplitude (CA) FCG curves. Because load interaction effects are neglected, this is an over simplification of reality. Better life predictions can be made if variable amplitude (VA) loading is considered. It is assumed that VA loading implies a sequence of varying amplitudes, where the order of various stress amplitudes is defined. Analyses completed show that CA loading can be unconservative, especially for cruise models. This is due to large amplitude loads placed upon the model system that are not modeled in the CA approach. VA loading accounts for the loading history, and may provide more accurate crack growth prediction. This would help achieve the project objective of identifying a more accurate and streamlined analysis method.

A load history from a specific NTF transport cruise performance model was considered typical of wind tunnel models and used to perform damage tolerance life predictions. When a cruise model is tested in the NTF, it typically begins each polar at a low AOA and steps up to higher AOA. These step increases in AOA increase the normal force acting on the model as seen in Figure 5. Figure 5 shows two time plots illustrating the progression of normal force for a typical test polar. Frequently a test polar ends with violent oscillatory loads associated with an unsteady separated flow condition, called pitch buffet, normally associated with large AOA. It is estimated that 30% of the 251 test polars ended with pitch buffet conditions.[25]

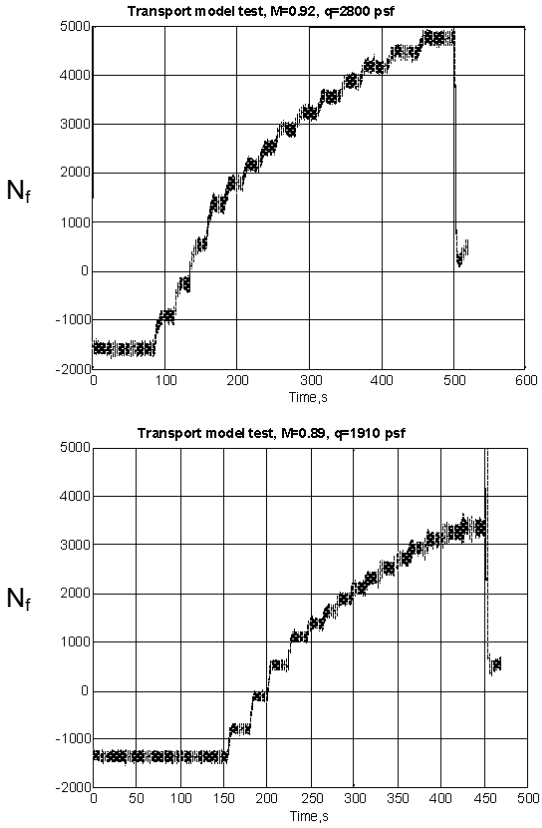

Figure 5 – Normal force data vs time.[25]

A stair stepped VA load spectrum was created to reflect the wind tunnel data for cruise model polar testing. For simplicity, the normal force was assumed to be the source of loading. It was assumed that pitch, yaw, and roll moments, and axial forces did not contribute to the fatigue process. The resulting load sequence of the transport model test then resembles the shape of the two plots of Figure 5 with 30% of the polars experiencing buffet loading. The varying amplitudes of loads can be observed as well as the oscillatory nature of the load sequence and

step increases in load due to increasing AOA. CA loading does not account for the pitch buffet loads. Pitch buffet is important to consider because large amplitude oscillations may overload the model and support hardware. Additionally, pitch buffet conditions produce significantly higher ΔK loads that significantly reduce the model fatigue life. Only by considering VA loading can the true load history, and its effects on fatigue life be described.

The step increases in load were calculated from data received from NTF tunnel operations.[25] VA load sequences are assumed proportional to normal force data taken from two test polars (M =0.89, q=1910psf and M =0.92, q=2800psf). These loads were used to predict stress at a specific location on the wing. Data was acquired at a high sampling rate, 320 Hz., creating an extremely large data set for each force component. This assumption is negligible in the case of the swept sting, where the normal force is completely dominant. The pitch moment is a minor load and again, dynamic loading is conservatively included in the balance data. Buffet onset (large amplitude oscillations) was also assumed to occur in 33% of the total polars. A plot of pitch buffet loads during a high Q test polar is shown in Figure 6.

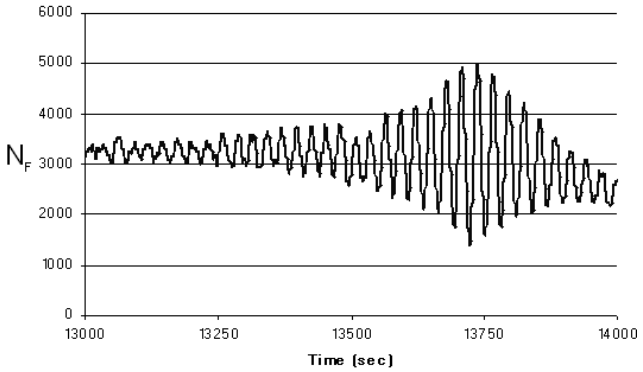

Figure 6 – Buffet region of high Q test polar.[25]

Comparison of FCG codes

Next each FCG code was used for life predictions on identical simple FCG scenarios. A surface flaw in the bottom of a trench (notch root) in a flat plate that was loaded by CA bending. Component dimensions and loads were obtained from an actual test specimen. Later, each FCG code will be compared with experimental results. Further, NDE techniques for in-service inspection were studied with these specimens. Experimental data (one specimen cycled to failure) provided a comparison of crack growth rates and specific crack lengths to evaluate the performance of FCG life predictions. Results produced by each of the FCG codes are plotted as crack length versus cycle count in Figure 7. Results from four of the codes are within 10% of each other. Because plane-strain-constraint and crack closure are considered, FASTRAN predicts a longer fatigue life. Neglecting these effects would produce results within the 10% range of the other four codes.

Simulation and results of NTF model problems

After the FCG codes were compared solving a simple problem, crack growth life predictions were conducted on two different parts of a typical NTF model configuration. One was the outboard screw wingtip attachment of a high aspect ratio wing transport model and the second was a swept strut sting design with a stress concentration at male taper joint fillet. The crack configuration of the wingtip attachment was modeled as a flat plate with a single corner crack at a hole. The crack configuration of the swept sting was modeled as a surface flaw in a solid rod. Crack configurations for the wingtip attachment and the swept sting are shown on the left and right sides of Figure 8, respectively. In reality, these structures are made from 200 grade maraging steel with a fracture toughness of approximately K_{Ic} = 68 ksi$\sqrt{}$in. Life predictions for both cases were made using each of the five FCG codes under both CA and VA load spectra previously discussed, and are listed in Table 2. For consistency, results (cycles) are reported in numbers of polars. That is, one cycle is equivalent to one polar (sequence of increasing AOA).

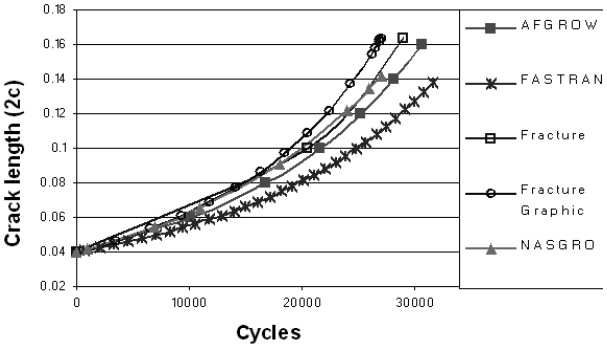

Figure 7 – Calibration plots of FCG codes.

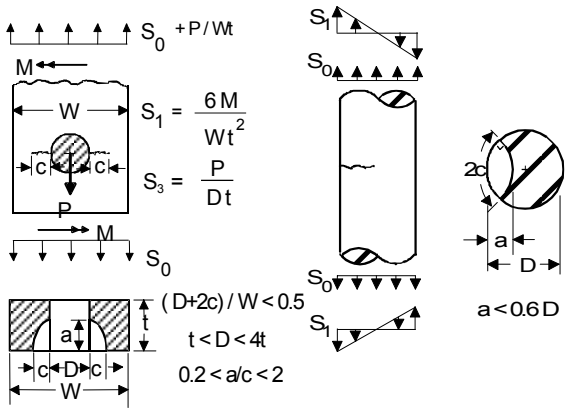

Figure 8 – Crack configurations for NTF model.[17]

For the wingtip attachment case, VA loading results in shorter fatigue crack growth life predictions (compared with CA loading) of 9% using NASGRO and 13.5% using AFGROW. Considering VA loading for the sting, predicted fatigue crack growth life decreased by 10% and 8.5% using NASGRO and AFGROW, respectively. Life predictions for VA loading were approximately 10% shorter than the corresponding CA cases. It is important to note that differences between fatigue life predictions of VA and CA loading is due to pitch buffet conditions where high amplitude oscillations occur. Pitch buffet conditions may occur at different test conditions and can vary in severity from polar to polar. Therefore, it is necessary to carefully monitor the dynamic loads for each polar. Previous fatigue life analyses use CA FCG data at R = 0.6 to model dynamic model loads. The data in figure 5 indicates that at buffet onset, the R is 0.3. Faster crack growth occurs at lower R ratios as shown in figure 2. The 10% reduction in life prediction between VA and CA loading has been attributed to this pitch buffet loading. Use of CA data may result in greater non-conservatism in life predictions where more (greater than average) pitch buffet loading occurs.

Table 2 – CA and VA FCG life predictions.

	Wingtip Attachment		Swept Sting	
FCG code	CA	VA	CA	VA
NASGRO	121,714	117,440	11,152	9,998
AFGROW	75,092	65,093	8,972	8,208
FASTRAN	120,000	63,258	N/A	N/A
FG	130,651	N/A	7,297	N/A

As previously shown, different FCG codes predict different fatigue lives although they all model the same problem. To predict FCG and fatigue lives with greater fidelity, it is important to consider load interaction effects, especially when considering VA loading and crack closure. Instantaneous FCG rate depends on current loading conditions as well as the load history.[18] NASGRO and AFGROW supply analysts with several empirical closure models to account for load history effects. These empirical models have adjustable parameters that must be chosen using experimental data. However, no analyses were performed using empirical data in this way.

Crack closure models like FASTRAN are well suited for VA loading and predicting FCG behavior with minimal empiricism. The primary drawback with VA load interaction models is that load history (blocks of CA cycles or a cycle-by-cycle load sequence) must be known. Generally, service loads are not well known by designers during model development. Another potential drawback is that retardation effects tend to increase the fatigue life making calculations potentially unconservative. Although safe operating conditions are maintained, model performance may be limited unnecessarily. Taking advantage of FCG retardation effects requires more complicated and computationally intensive modeling efforts. However, the more accurate prediction that may be obtained from a crack closure model and VA loading outweighs the additional effort. Ultimately, load data could be acquired during each wind tunnel test and used for damage tolerance life prediction. In this way, a cumulative damage analysis can be performed (preferably in concert with NDE verification) to predict or monitor fatigue lives of any wind tunnel model.

NON-DESTRUCTIVE EVALUATION (NDE)

In terms of effects on fatigue life predictions, the assumption of an initial crack size is extremely influential. The damage tolerance methodology is inherently conservative because if no initial flaw can be detected (*i.e.* a pristine new part), the smallest crack that cannot be reliably detected is assumed to exist. It has been standard practice to make models from material that has passed NDE examinations and contain no cracks greater than a $^1/_{64}$" diameter flaw.[26] However, obtaining materials of this quality is difficult and the NTF has been forced to accept lower quality material where no flaw greater than or $^3/_{64}$" diameter exists. Further, inspection experience at LaRC indicates that initial flaws are more likely a result of machining than manufacturing. This indicates NDE inspection should be done on the final machined model

instead of the as-received raw material as emphasized by current procedures. NDE tests are infrequently performed on finished models and are done at the discretion of the technical project engineer or facility safety head.

Recent advances in NDE technology are changing inspection thresholds for small fatigue cracks. The final task in this project is to evaluate the usefulness of NDE methods in a damage-tolerance-life-monitoring scheme for NTF models. High resolution radiographic (X-ray) and eddy current techniques are possible NDE techniques that may be studied in the future. The NDE efforts discussed here are limited to ultrasonic and eddy current crack detection methods. Non-linear ultrasonic techniques are promising for detecting fatigue pre-cracking in in-service (*i.e*. while in use) models. Some difficulty is expected relating to calibration (*i.e*. interpretation) of ultrasonic data. Fatigue cracks about chordwise wing pressure tube troughs (common features in wind tunnel models) are a geometry of specific interest where NDE ultrasonic techniques will be evaluated.

NDE In-service technique

NTF wind tunnel models typically have an array of small orifice tubes embedded in their aerodynamic surfaces to measure pressure. These tubes are routed through the aerodynamic surfaces by collector troughs and are machined into the surface to a central pressure transducer. Once filled with tubes, these troughs are potted with a polymer material and contoured to match the adjacent profile. The collector troughs present a formidable inspection challenge in that, once filled, they are completely obscured for all surface inspections (*e.g*. dye penetrant). If a crack or other defect initiates at the bottom of the trough, it will be difficult to detect and measure. It is possible that a defect so situated could grow to failure before a visible on the surface. Because of stress concentrations about pressure tubes and troughs, fatigue cracks initiation may be especially likely at these sites.

To evaluate ultrasonic crack detection techniques, plates of Vascomax-200 steel were machined with a trough approximately 50% of the plate depth and perpendicular to the loading axis. A small notch was machined at the bottom of the trough (notch root) in the center of the specimen. Specimens were loaded and fatigue cracks initiated at the starter notch. Specimens were tested (at CA loading) with and without tubes potted in the trough to simulate operating conditions in NTF models. Different specimens were used to develop suitable inspection techniques for crack detection, monitoring FCG, and measuring crack depth.

The ability to reliably detect small cracks below the trough collector tubes and filler material was initially thought to be unachievable. Efforts were focused on solving the immediate problem of small defect detection and sizing. Initial work was done to evaluate the application of electromagnetic (eddy current) inspection technology for this task. Experiments with multiple coil types and frequencies were universally unsuccessful at detecting either the starter notches or subsequently grown cracks. A best-fit coil was designed and procured in an attempt to achieve detectability. This also was unsuccessful.

Success was achieved through the use of an adapted and miniaturized ultrasonic defect technique. During the mid-1980s the Electric Power Research Institute (EPRI) developed an ultrasonic technique for detecting and measuring intergranular stress corrosion cracks in nuclear power generation facilities. This technique took advantage of signal diffraction and reflection about small crack tips. Here, the crack tip acts like a point radiator that generates a small diffracted signal. The crack also reflects a stronger signal from its surface interface as shown schematically in Figure 9.

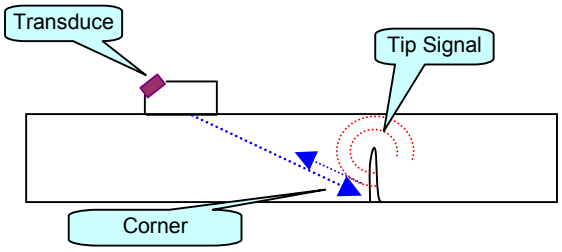

Figure 9 – Corner reflection/detection geometry.

If the timing relationship (relationship between reflection time and crack depth) is known, accurate crack measurements can be made. As developed by EPRI, this technique relied on large (0.5" – 1" diameter) transducers with limited accuracy. Recent technological improvements have led to smaller transducers and greater accuracy in crack detection.

For experiments described here, a subminiature angle-beam ultrasonic transducer (Krautkramer – SMSWS) with a center frequency of 15 MHz, $^{1}/_{8}$"

effective diameter, and a 70° beam angle was used. A digital ultrasonic instrument (Krautkramer USD-15) was also used. The detection and measurement of small cracks necessitated manufacturing a test reference part (*i.e*. part without a fatigue crack or starter notch) as shown in Figure 10.

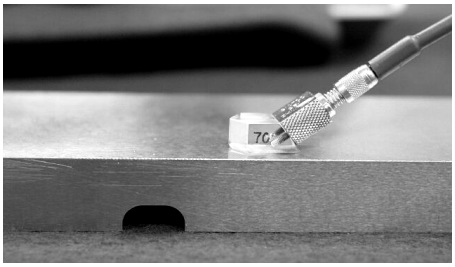

Figure 10 – Geometry of transducer and trough.

To mimic the crack tip reflector, a series of square notches with known depth were machined in a test bar. The ultrasonic corner and tip signals from these notches were recorded and a timing relationship established. A timing relationship plot was generated from the notch data for use during the FCG study as shown in Figure 11.

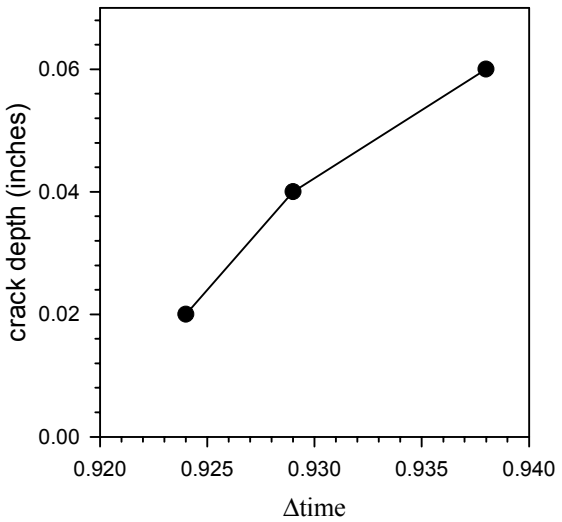

Figure 11 – Crack depth vs reflection time.

Crack detection was done by placing the transducer opposite the trough as shown in Figure 10. The transducer was oriented with the central sound beam perpendicular to the trough axis. Maintaining this orientation, the transducer was moved parallel to the trough to detect the cracks. This process was designed to minimize ultrasonic reflections of the trough. The transducer was skewed or fanned as it was moved down the trough. Crack signals were transient in nature during scanning. Once signal was detected that indicated a small crack was present, the transducer was manipulated to achieve the best possible response signal (*i.e*. peak amplitude of the reflection). The signal time and amplitude was then compared to known data (see Figure 11) to determine its size and location. Both crack detection and measurements were found to be accurate during the FCG tests and subsequent post-failure inspections. The adaptation of this ultrasonic detection method to actual NTF models is reasonable. A photo of a finished test specimen with tubes potted in the trough is shown in Figure 12.

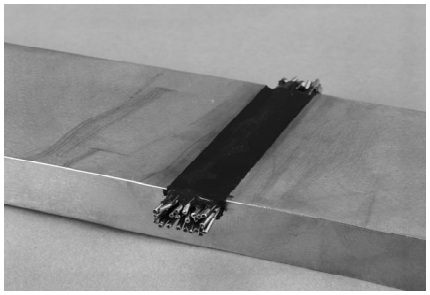

Figure 12 – Trough geometry.

In summary, the NDE process should be performed initially and periodically during the service life. This, along with a damage tolerant approach to fracture mechanics, will provide a method to increase test article structural performance and safety. These tools can provide safety during testing at conditions above the loads currently analyzed for in NTF models.

CONCLUSIONS

Two materials were found to be suitable alternative alloys for NTF wind tunnel models; Aermet 100 and Vascomax C250. Aermet 100 is slightly superior to C250 due to higher fracture toughness. FCG and fracture properties have been obtained, or will be obtained in the future, to facilitate damage tolerance analyses. Five different FCG codes were evaluated as life prediction tools under both CA and VA loading. Typically, using CA load specta results in life predictions that are 10% greater than for VA load spectra. Differences between life predictions made with CA and VA load specta are attributed pitch buffet loads, which are neglected by CA spectra. Finally, an in-tunnel crack detection technique using NDE ultrasonic techniques was

studied. Cracks were successfully detected and sized in the bottom of pressure tube trenches from the opposite side of the specimens.

Several tasks are planned for future study and are described below.

- Use of real time loads in a damage tolerance life monitoring system. The effects of severe loading on safe fatigue life could be determined before each test.
- Develop or refine current NDE techniques for crack detection/monitoring of NTF models. Information about fatigue crack damage could be made available before, or even during, testing.
- Revise the LaRC guidance document, LAPG 1710.15 Wind tunnel models criteria to include use of a generalized FCG curve for all maraging steels and use of VA load spectra for damage tolerance life predictions.

ACKNOWLEDGEMENTS

The project involved personnel from several organizations at LaRC within a multidisciplinary team. The contributions of Jim Newman at Dick Everett in the Mechanics of Durability Branch at LaRC are greatly appreciated. As well as the support from the Non-destructive Evaluation Systems Branch at LaRC.

REFERENCES

[1] Wind Tunnel Model Systems Criteria, LAPG1710.15, NASA Langley Research Center, September 2000.

[2] Tobler, R.L., "Materials Studies for Cryogenic Wind Tunnels", National Bureau of Standards, NBSIR 79-1624, 1980.

[3] Wigely, D.A., "ETW Materials Guide", ETW GmbH, ETW/D/95005, 1996.

[4] Rush, H. F., "Grain-Refining Heat Treatments to Improve Cryogenic Toughness of High Strength Steels," NASA TM-85816, 1984.

[5] Wigely, D.A., "The Dimensional Stability Analysis of Seventeen Stepped Specimens of 18Ni 200 Grade, PH13-8Mo and A-286", NASA Contractor Report CR-172168, 1983.

[6] Suresh, S., Fatigue of Materials, Cambridge University Press, 1991, Cambridge, UK.

[7] Everett, R. A. and Elber W., "Damage Tolerance Issues Related to Metallic Rotorcraft Dynamic Components," *Journal of the American Helicopter Society*, v. 45, pp. 3-10.

[8] Fracture Technology Associates, User's Reference Manual for Automated Fatigue Crack Growth (Compliance), v. 2.43, Fracture Technology Associates, Bethlehem, PA.

[9] Saxena, A., Hudak, S. J., Donald, J. K., and Schmidt, D. W., "A computer controlled decreasing stress intensity technique for low rate fatigue crack growth testing," Journal of Testing and Evaluation, v. 6, 1978, pp. 167-174.

[10] McClung, R. C., "Analyses of Fatigue Crack Closure During Simulated Threshold Testing," Fatigue Crack Growth Thresholds, Endurance Limits, and Design, ASTM STP 1372, ASTM, West Conshohocken, PA, pp. 209-226.

[11] Newman, J. C., "Analyses of Fatigue Crack Growth and Closure Near Threshold Conditions for Large-Crack Behavior," Fatigue Crack Growth Thresholds, Endurance Limits, and Design, ASTM STP 1372, ASTM, West Conshohocken, PA, pp. 227-251.

[12] Donald, J. K., Bray, G. H., and Bush, R. W., "Introducing the K_{max} Sensitivity Concept for Correlating Fatigue Crack Growth Data," High Cycle Fatigue of Structural Materials, The Minerals, Metals, and Material Society, 1978, pp. 123-141.

[13] Wagner, J.A., "Mechanical Behavior of 18 Ni 200 Grade Maraging Steel at Cryogenic Temperatures", AIAA-85-0704, 1985.

[14] "Cryogenic Wind Tunnel Models design and fabrication", NASA-CP-2262, 1983.

[15] Paris, P. C. and Erdogan, F., "A Critical Analysis of Crack Propagation Laws," Journal of Basic Engineering, 1963, pp. 528-534.

[16] Forman, R.G., Henkener, J.A., Lawrence, V.B., Williams, L.C., "Derivation of Crack Growth"

[17] NASGRO,*Computer software for Win9x/NT/2000* ,http://mmptdpublic.jsc.nasa.gov/nasgro/nasgromain.html, NASA Johnson Space Center, 2000.

[18] Anderson, T.L., "Fracture Mechanics: Fundamentals and Applications", CRC Press, 1995.

[19] Broek, D., "Elementary Engineering Fracture Mechanics", Fourth Edition, Nijhoff, 1985.

[20] AFGROW, *Computer software for Win9x/NT/2000* ,http://fibec.flight.wpafb.af.mil/fibec/afgrow.html, Wright Patterson Air Force Base, 2000.

[21] Newman, J.C., "FASTRAN-II – A Fatigue Crack Growth Structural Analysis Program," NASA TM-104159, LaRC, 1992.

[22] FRACTURE, *A LaRC in-house PC software code for fracture analysis and life prediction*, Dr. C. Michael Hudson and Mr. Charles V. Dunton.

[23] FractureGraphic, *A commercial PC software code.* http://www.srt-boulder.com, SRT Inc. Boulder, Co., 2000.

[24] "Properties of Materials for NASA/FLAGRO 2.0," JSC-26254, NASA-JSC, Houston, TX, June 1994.

[25] Balakrishna, S., "Assessment of Life Cycle for Typical Cruise Test at NTF and Load Spectrum During the Test Cycle", unpublished work, LaRC NTF, Vigyan Inc., 2000.

[26] Berry, R.F., "Fabrication Division Ultrasonic Inspection Specification for Critically Stressed Components", NASA TM-84625, 1983.